PROTEINS: Structure, Function, and Bioinformatics 55:502–507 (2004)

Polyproline II Helix Is the Preferred Conformation for Unfolded Polyalanine in Water

Mihaly Mezei,[1]* Patrick J. Fleming,[2] Rajgopal Srinivasan,[3] and George D. Rose[2]*
[1]*Department of Physiology and Biophysics, Mount Sinai School of Medicine, New York University, New York, New York*
[2]*Jenkins Department of Biophysics, Johns Hopkins University, Baltimore, Maryland*
[3]*Tata Consultancy Services, Hyderabad, India*

ABSTRACT **Does aqueous solvent discriminate among peptide conformers? To address this question, we computed the solvation free energy of a blocked, 12-residue polyalanyl-peptide in explicit water and analyzed its solvent structure. The peptide was modeled in each of 4 conformers: α-helix, antiparallel β-strand, parallel β-strand, and polyproline II helix (P_{II}). Monte Carlo simulations in the canonical ensemble were performed at 300 K using the CHARMM 22 forcefield with TIP3P water. The simulations indicate that the solvation free energy of P_{II} is favored over that of other conformers for reasons that defy conventional explanation. Specifically, in these 4 conformers, an almost perfect correlation is found between a residue's solvent-accessible surface area and the volume of its first solvent shell, but neither quantity is correlated with the observed differences in solvation free energy. Instead, solvation free energy tracks with the interaction energy between the peptide and its first-shell water. An additional, previously unrecognized contribution involves the conformation-dependent perturbation of first-shell solvent organization. Unlike P_{II}, β-strands induce formation of entropically disfavored peptide:water bridges that order vicinal water in a manner reminiscent of the hydrophobic effect. The use of explicit water allows us to capture and characterize these dynamic water bridges that form and dissolve during our simulations. Proteins 2004;55:502–507.** © 2004 Wiley-Liss, Inc.

Key words: polyalanine; polyproline II; free energy; Monte Carlo

INTRODUCTION

Unfolded proteins are usually thought to be featureless, random coil polymers,[1,2] with a negligible energetic preference for any particular conformation. During the folding reaction, U(nfolded) ⇆ N(ative), water is stripped from the polypeptide backbone, and upon completion, little (if any) structural water remains in the interior of the folded protein. Consistent with random coil statistics, it is often assumed that the backbone is uniformly solvated in the unfolded state and that the energy of solvent stripping does not vary systematically from one residue to another, although see Avbelj and Baldwin.[3,4]

We tested this assumption with model peptides in explicit water[5] using free energy simulations.[6,7] Specifically, the solvation free energy was computed for a 12-residue polyalanyl-peptide with blocked termini (*N*-Acetyl-Ala_{12}-*N′*-Methylamide) in each of four representative conformers: α-helix, antiparallel β-strand, parallel β-strand, and left-handed polyproline II helix (P_{II}). These four conformers represent the four main sterically allowed regions for the alanyl dipeptide. The water structure surrounding each conformer was then analyzed in detail. The conventional nomenclature can be misleading: P_{II}, a left-handed helix with a pitch of exactly 3 residues per turn, is the sterically forced conformation for polyproline,[8] but proline-free peptides can also adopt this conformation. Polyalanine can be regarded as an effective model for the polypeptide backbone.

Remarkably, we find that solvation free energy favors P_{II} over β-strands or α-helix. This conformation-dependent difference in solvation will contribute importantly to preorganization in the unfolded state of both peptides and proteins. The observed entropy loss on folding is usually thought to measure a reduction in the number of distinct unfolded states, but we show that it could also be explained by a reduction in the degeneracy of a single state.

METHODS

Detailed descriptions of all methods have been published previously. The solvation free energies of 4 conformers of interest were calculated by extending an 11-mer into the corresponding 12-mer using thermodynamic integration, under the plausible assumption that short-range end effects will cancel in peptides of this length.

In both experiments and simulations, free energy is typically determined by accessing some derivative and integrating appropriately. Unlike experiments, such integration need not be constrained to follow a physical path in simulations; any thermodynamic variable that is a function of the potential energy will serve.

Grant sponsor: National Institutes of Health; Grant sponsor: Mathers Foundation.

*Correspondence to: George D. Rose, Department of Biophysics, Johns Hopkins University, 3400 N. Charles Street, Baltimore MD 21218. E-mail: grose@jhu.edu; and Mihaly Mezei, Department of Physiology & Biophysics, Mt. Sinai School of Medicine, One Gustav Levy Place, Box 1218, New York, NY 10029. E-mail: mezei@inka.mssm.edu

Received 14 August 2003; Accepted 23 September 2003

Published online 5 March 2004 in Wiley InterScience (www.interscience.wiley.com). DOI: 10.1002/prot.20050

TABLE I. Conformation-Dependent Solvation Parameters

	$\Delta A_{solvation}$	Area	V_{FS}	$\Delta\|\mu\|$	K_{FS}	ρ_{FS}	E_{FS}	E_{FS}^{WW}
Helix	−2.0 ± 0.3	65	3681 ± 1	0.76	79.6 ± .7	0.65 ± .01	−105.2 ± 1.6	−3.36 ± 0.02
P_{II}	−4.7 ± 0.3	100	4539 ± 1	0.48	114.8 ± .7	0.76 ± .06	−193.4 ± 2.4	−3.29 ± 0.02
Parallal-β	−3.9 ± 0.3	111	4748 ± 1	0.55	118.4 ± .7	0.75 ± .00	−162.8 ± 2.1	−3.28 ± 0.02
Anti parallal-β	−4.0 ± 0.3	114	4817 ± 1	0.32	120.1 ± .7	0.75 ± .00	−160.0 ± 2.2	−3.26 ± 0.02

$\Delta A_{solvation}$ is the Helmholtz free energy of solvation per residue in kilocalories per mole, obtained as $\Delta A_{solvation}$ (11 → 12), the free energy difference between a 12-mer and an 11-mer.
Area is the solvent-accessible surface area per residue in Ångstrom units squared.
V_{FS} is the volume of the first solvent shell in Ångstrom units cubed.
K_{FS} is the number of water molecules in the first solvent shell.
ρ_{FS} is the density of the first solvent shell, $\langle K_{FS}\rangle/V_{FS}$, converted to gm/ml.
E_{FS} is the solvation energy of the first solvent shell, in kilocalories per mole.
E_{FS}^{WW} is the water:water pair energy for first-shell waters, in kilocalories per mole.
$\Delta|\mu|$ is the dipole moment change from an 11-mer to a 12-mer, in Debye.

Among the options for calculating solvation free energy differences from simulations,[7,9–11] thermodynamic integration on a polynomial path was chosen because it is particularly well suited to changes involving the creation of new atoms.[12,13] The method is a generalization of the "nearly linear path"[6,7]; it leads to a very smooth path and therefore scales well with increasing solute size.

Simulations were performed in the canonical ensemble with the MMC program[14] at a temperature of 300 K, using the Metropolis algorithm[15] with force-bias sampling,[16] modified to reduce the λ factor of force-biasing near the solute.[17] The CHARMM 22 force field[18] was used, with peptides surrounded by TIP3P[5] water. All-atom representations of blocked, polyalanyl peptides were modeled in α-helix ($\phi = -64°$, $\psi = -43°$) with 2201 waters, antiparallel β-strand ($\phi = -139°$, $\psi = 135°$) with 2751 waters, parallel β-strand ($\phi = -119°$, $\psi = 113°$) with 2528 waters, and P_{II} helix ($\phi = -78°$, $\psi = 149°$) with 2655 waters. The frequency of attempted moves was increased near the solute using the preferential sampling technique of Owicki.[19] Periodic boundary conditions were adopted to approximate a condensed phase environment, using a cell that resulted in the smallest number of waters for comparable image–image distances, as determined by the program Simulaid.[20] The solute was held rigid during each simulation.

Solvent structure analyses were based on simulations of 10^8 Monte Carlo steps, preceded by 25×10^6 equilibration steps. Each step involved an attempt to move one water molecule. Mean solute–solvent and solvent–solvent energies, first-shell volumes, coordination numbers, solute–solvent radial distributions, and orientational correlations were determined using proximity analysis.[21] In particular, the first solvation shell of peptide atoms comprises those solvent atoms around the peptide within an atom type-dependent distance of 5.3 Å, 3.3 Å, 3.3 Å, and 2.2 Å for C, O, N, and H atoms, respectively. The first-shell solvation energy, E_{FS}, includes the interaction between waters in the first shell and the entire peptide. Solute:water interactions were calculated under the minimum image convention; distances are between the centers of neutral groups. Water:water interactions were calculated using a 10 Å spherical cutoff; distances are between the centers of mass.

RESULTS

The solvation free energy of P_{II} is favored over both β-strand conformers by ~0.7 kcal/mol/residue, and over α-helix by 2.7 kcal/mol/residue (Table I). In the α-helix, 8 amide hydrogens and carbonyl oxygens form intrasegment hydrogen bonds,[22] which affect their interaction with solvent. However, the 3 extended conformers—P_{II}, parallel β-strand, and antiparallel β-strand–cannot make intrasegment hydrogen bonds, yet their solvation free energies differ significantly.

These differences defy conventional explanation (Table I). The volume of the first solvent shell around each residue scales linearly with its solvent-accessible surface area in all 4 conformers, and with almost perfect correlation; but neither of these quantities is correlated with solvation free energy. Nor do the calculated solvation free energies correlate with the change in the dipole moments of the 3 extended conformers. Further, the number of water molecules in the first solvent shell is approximately the same for all 3, and the slight difference between P_{II} and the β-strands is anticorrelated with their solvation free energy. Similarly, solvent density in the first solvent shell is the same for all 3.

None of these terms is sufficient to rationalize the observed differences in solvation free energy. However, the first-shell solvation energy, E_{FS}, correlates with $\Delta A_{solvation}$ almost perfectly (Table I). In addition, contributions arising from the presence of entropically disfavored water bridges in β-strands may also be important, as described in the next section.

It is evident that solvent-exposed peptide polar groups can hydrogen-bond to water readily in all conformations: in 4001 "snapshots" from the 10^8 Monte Carlo steps (1 snapshot every 25,000 steps), the average number of peptide:water hydrogen bonds per residue, are 0.56, 1.42, 1.28, and 1.17 in α-helix, P_{II}, parallel β-strand, and antiparallel β-strand, respectively. Among the 3 extended conformers, the distribution of hydrogen-bonded water molecules along the peptide is approximately uniform. In contrast, a nonuniform distribution of hydrogen-bonded water molecules is observed in the α-helix. Although water:peptide hydrogen bonding is curtailed for groups that participate in intrasegment hydrogen bonds, some

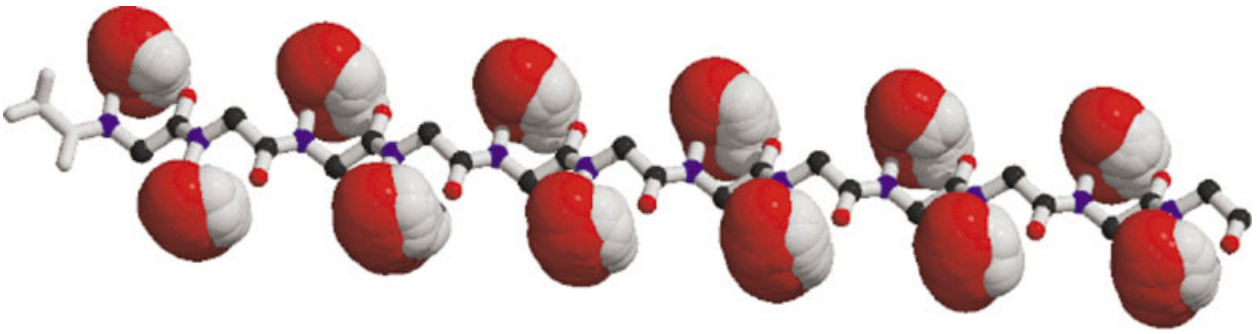

Fig. 1. Water forms bridges readily with β-strands. The figure shows an antiparallel β-strand (ball-and-stick, backbone atoms only) on which 911 bridging waters (CPK, hydrogen-bonded O-Hs only) from multiple simulation "snapshots" have been superimposed. Specifically, the total of 10^8 Monte Carlo steps was sampled every 25,000 steps. Bridging waters in each sample were extracted, collected, and are shown superimposed in the figure. Conventional CPK colors are used: red, oxygen; blue, nitrogen; black, carbon; white, hydrogen. Water bridges are dynamic and short-lived, but in the aggregate, they form tightly clustered bridges, doubly hydrogen-bonded to each peptide's carboxyamide.

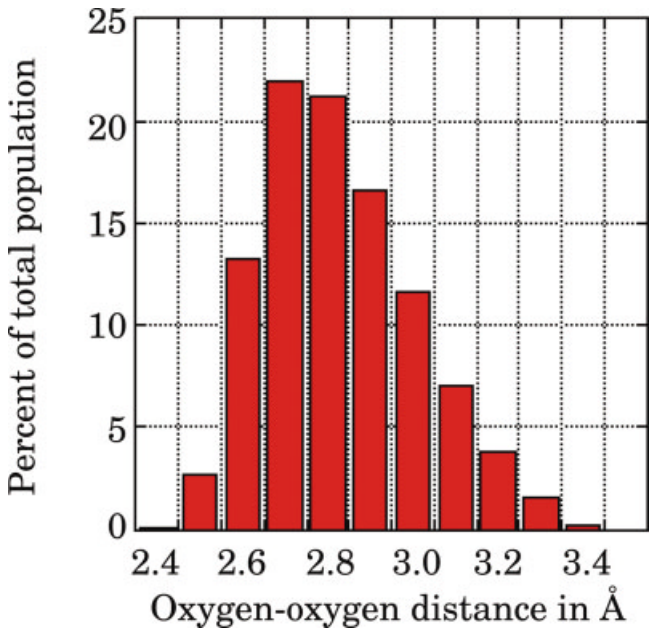

Fig. 2. Distribution of oxygen–oxygen distances in adjacent water molecules taken from 50 boxes of equilibrated TIP3P water,[5] 300 water molecules per box. Longer chains have broader distributions.

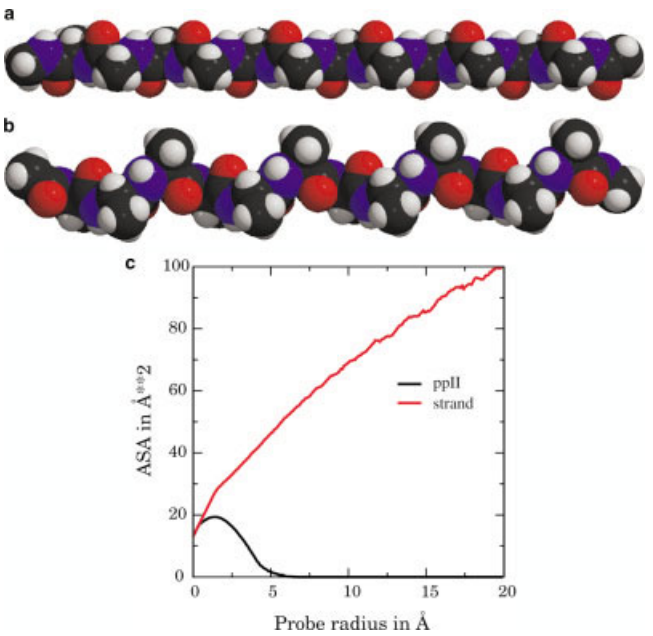

Fig. 3. Water bridges are incommensurate with P_{II} geometry but not with β-strand geometry. In β-strands, carbonyl oxygen atoms are situated on a convex surface of the peptide (**a**), where they are accessible to water; in P_{II}, these atoms are on a concave surface of the peptide (**b**), where they are sequestered from water. This structural difference can be quantified by plotting the solvent accessible surface area[23] of the backbone carbonyl oxygen as a function of probe size (**c**) for β-strands and P_{II}. Strands (red curve) and P_{II} (black curve) exhibit opposite behavior: As probe size increases, area increases in β-strands but decreases in P_{II}.

water:O═C hydrogen bonding is still present. In all cases, the number of peptide:water hydrogen bonds is smaller than the corresponding coordination number, indicating that some proximate water molecules are not hydrogen-bonded to the peptide. Importantly, there are more hydrogen-bonded water molecules around both NH and C═O groups in P_{II} than in either β-strand conformer.

Water bridges. Differences in conformation can also induce corresponding differences in solvent entropy by disrupting solvent organization. To explore this phenomenon, we analyzed the 4001 snapshots for water bridges. A *water bridge* is defined as a water molecule that is doubly hydrogen-bonded to the peptide, at both a >NH and a >C═O. Such bridging isolates water molecules from the bulk solvent phase. Notably, water can form bridges readily with β-strands (Fig. 1), but P_{II} geometry is incommensurate with bridge formation. Among the 4001 snapshots, we found 911 water bridges in antiparallel β-strands, 507 in parallel β-strands, and none in either P_{II} or α-helix.

These water bridges in strands are entropically disfavored, because bridging disrupts the hydrogen-bonding network of the bulk phase. Longer bridges—consisting of 2 or more waters—also occur, but surprisingly, these can be accommodated readily because the equilibrium distribution of donor-to-acceptor distances in longer water chains is quite broad, and corresponding acceptor-to-donor distances in the peptide are within this distribution (Fig. 2).

Relevant differences in peptide geometry are illustrated in Figure 3. Carbonyl oxygen atoms in β-strands are situated on an accessible convex surface of the peptide [Fig. 3(a)], whereas carbonyl oxygens in P_{II} are on a sequestered concave surface [Fig. 3(b)] that limits water orientation. These differences can be quantified by plotting the solvent-accessible surface area[23] of the backbone carbonyl oxygen as a function of probe size [Fig. 3(c)].

In comparison to P_{II}, β-strands not only pay a larger price in solvent entropy but also derive a smaller gain in solvent energy, as reflected in both their reduced energy of interaction with the first solvent shell (Table I) and smaller number of peptide:water hydrogen bonds (see above). *In essence, water is simply a better solvent for P_{II} than for strands*.

DISCUSSION

Thermodynamics of Solvation/Desolvation

According to Edsall and McKenzie,[24] "Water is unique among the known liquids or almost so," and its solution thermodynamics are complex and incompletely understood. At physiological temperature, pure water comprises a completely interconnected network of hydrogen-bonded molecules. We tested this assertion using 50 boxes of 300 TIP3P water molecules, extracted from a simulation of 5×10^6 Monte Carlo steps under the same conditions as our peptide simulations. A molecule was selected at random from every box, and its hydrogen-bonded lattice was traversed. In each case, the lattice included all waters in the box, with the exception of at most 3 singletons.

Naively, it might be expected that a fluctuation could propagate throughout the network in such an interconnected system. In fact, perturbative effects are typically local, dying away beyond the first solvent shell surrounding the perturbant.[25]

One can define 4 categories, divided somewhat arbitrarily into (i) apolar and (ii) polar solutes in water, and isolated water molecules in (iii) apolar and (iv) polar compounds:

(i) Strong correlations between water and small apolar solutes (e.g., argon, methane, residue sidechains) comprise the hydrophobic effect,[26] itself complex and entropy-driven at physiological temperature,[27] but enthalpy-driven at higher temperatures.[28]

(ii) Strong interactions between water and small polar solutes (e.g., ions, hydrates of inorganic salts, model amides) are mainly enthalpic: See Table 1 in Avbelj et al.[29] Water molecules reorganize around the polar moiety with a comparatively small loss of conformational entropy.[30]

(iii) Water molecules isolated from the bulk and transferred into an apolar environment (e.g., a hydrophobic cavity in a protein) can gain entropy[31] owing to increased liberational freedom, akin to transfer from solution to the gas phase.

(iv) Finally, water molecules isolated from the bulk and transferred into a multiply hydrogen-bonded polar environment (e.g., a 3_{10}-helix[32]) would be expected to lose both rotational and translational entropy.

The favorable interaction energy between P_{II} and solvent (E_{FS} in Table I) corresponds to category (ii), while the water bridges that form around β-strands correspond to category (iv). In effect, a β-strand is a water-organizer, in that it promotes an entropically disfavored redistribution of its vicinal water.

An α-helix is also a water-organizer, as shown in Table I. Intrasegment hydrogen bonds raise $\Delta A_{solvation}$ in comparison with the other conformers and promote water:water interactions, as reflected in stronger E_{FS}^{WW} values.

In summary, our simulations show that P_{II} structure is favored over other conformers because its geometry is commensurate with lower solvation energy and higher solvation entropy.

Polyproline II and the Unfolded State of Proteins

Our previous study[33] showed that P_{II} conformation is favored in short polyalanyl chains when self-interactions are minimized with respect to soft-sphere repulsion (the repulsive part of a Lennard–Jones 6-12 potential). In essence, favorable chain entropy (i.e., "wiggle room") in P_{II} exceeds that in β-strands or α-helices. Explicit solvation effects were not included in this earlier study, but minimizing chain:chain interactions implicitly maximizes chain:solvent interactions.

The present study is complementary, focusing on solvation free energy in explicit water. From these two studies, we conclude that both chain:chain and chain:solvent interactions favor P_{II} conformation in short polyalanyl peptides. The accompanying paper by Kentsis et al.,[34] which characterizes the unfolded ensemble of short polyalanine chains in water including both peptide:peptide and peptide:water interactions, also finds an abundant population of P_{II} helices with persistence lengths of 4–5 residues.

Using a combination of circular dichroism (CD) and NMR, Shi et al.[35] showed that a sequence having 7 consecutive alanine residues is predominantly P_{II} at 2°C, with β-strand content increasing by ~10% at 55°C. A significant unfavorable enthalpy—estimated to be ~3 kcal/mol/residue—is associated with this thermal transition. This enthalpy value is approximated by ΔE_{FS} between P_{II} and β-strand (193 − 161 kcal/mol/12 residues = 2.66 kcal/mol residue) in Table I, suggesting that the effect measured by Shi et al.[35] is mainly an enthalpy of solvation.

Water bridges in β-strands are estimated to contribute a much smaller fraction to differences in $\Delta A_{solvation}$. A bridge was found in approximately 25% of the 12-residue antiparallel β-strands (i.e., ~2% of the residues have bridges). From hydrates of salts, Dunitz[30] bracketed the entropic cost of a bound water molecule between 0–7 cal/mol/K, corresponding to a free energy cost of 0–2 kcal/mol at 300 K. At the upper extreme, this sums to an entropic cost of only ~0.04 kcal/mol for the peptides simulated here. However, the energy difference, ΔE_{FS}, between P_{II} and β-strand, noted above, is 2.66 kcal/mol/residue, whereas the corresponding free energy difference, $\Delta A_{solvation}$, is only 0.7 kcal/mol/residue, so additional differences in solvent organization may play an important role. In particular, our values of ΔE_{FS} do not include the solute-induced

energy of solvent reorganization. E_{FS} for second-shell waters was also calculated (data not shown); here, the energy favors P_{II} over β-strands by only ~0.17 kcal/mol/residue. Thus, the factors of interest are realized largely with the first solvent shell.

A survey of proteins from the Protein Data Bank (PDB)[36] found that P_{II} helices are rare in folded proteins, although individual residues often adopt ϕ,ψ-angles with P_{II} values.[37] Why is P_{II} helix favored in the unfolded state but disfavored in the native state? The likely reason involves hydrogen bonding. Upon folding, most backbone polar groups are disposed to the interior of the protein, where they form intramolecular hydrogen bonds to compensate for lost hydrogen bonds with bulk water; uncompensated polar groups are extremely unfavorable and seldom found.[38] However, P_{II} helices can form neither intra- nor intersegment hydrogen bonds with other elements of regular secondary structure. Consequently, the hydrogen-bonding requirements of folded proteins are incompatible with the persistence of P_{II} helices.

Conformational Entropy and the Unfolded State—a Reassessment

If P_{II} is a dominant conformation in polyalanyl peptides, then it is also likely to be favored in unfolded proteins.[39] If so, the unfolded state is not as heterogeneous as previously believed.[33] The usual estimate of ~5 accessible states per residue in an unfolded protein is based on a familiar argument: The free energy difference between the folded and unfolded populations, ΔG_{conf}, is a small difference between large value of ΔH_{conf} and $T\Delta S_{conf}$.[40,41] If $\Delta G_{conf} \approx -10$ kcal/mol (a typical value) and $\Delta H_{conf} \approx 100$ kcal/mol, then the counterbalancing $T\Delta S_{conf}$ is also ≈100 kcal/mol. Then $\Delta S_{conf} \approx 3.33$ entropy units per residue for a 100-residue protein at 300 K. Assuming $\Delta S_{conf} = R \ln W$, the number of states per residue, W, is 5.34.

However, instead of a reduction in distinct states, *the entropy loss on folding could result from reducing the degeneracy of a single state*. In particular, the ϕ,ψ-space of occupied regions in the unfolded population would be constricted upon folding. For example, using the $\Delta A_{solvation}$ values in Table I, a residue in P_{II} is within an ambient-temperature fluctuation of any sterically allowed ϕ,ψ-value in the northwest quadrant of the dipeptide map. Consequently, different ϕ,ψ-values from these regions would be thermodynamically indistinguishable, and therefore not distinct states at all. As a back-of-the-envelope approximation, consider a residue that can visit any allowed region of the NW quadrant in the unfolded state. Upon folding, let this residue be constrained to be within ±30° of ideal β-sheet ϕ,ψ-values. The reduction in ϕ,ψ-space would be a factor of 5.58 (see Fig. 1 in Pappu et al.[42]), close to the typical value attributed to distinct states. Similar, but less approximate, estimates can be obtained when the unfolded populations are Boltzmann-weighted (e.g., see Figs. 5 and 6 in Pappu and Rose[33]).

Related Studies

More than three decades ago, Tiffany and Krimm[43] hypothesized that a substantial P_{II} population exists in unfolded proteins, a prescient conclusion based on observed similarities between the CD spectra of proline homopolymers and denatured proteins. Lately, Creamer and coworkers[8,37,44–46] have analyzed P_{II} conformation extensively, in both solution and calculations. Other simulations have also been performed at the detailed atomic level in explicit water. In Monte Carlo simulations, Kentsis et al.[34] find P_{II} helices to be approximately isoenergetic with β-strands. Using replica exchange molecular dynamics, Garcia[47] observed a striking water channel surrounding the P_{II} backbone. A dominant P_{II} population is also found in similarly motivated calculations using implicit solvent models.[48,49] Experimental studies as well find P_{II} to be the favored conformation in both a dipeptide[50] and a heptapeptide.[35] Indeed, the prevalence of P_{II} conformation is a pervasive theme that runs throughout a recent volume on unfolded proteins.[39] Very recently, Hinderaker and Raines[51] showed that electronic effects ($n \rightarrow \pi^*$) also favor P_{II}.

In three fundamental articles that merit particular attention, Avbelj and Baldwin re-evaluated the solvation energetics of the peptide group.[3,4,29] Their investigations began with the surprising observation that the familiar numbers for α-helix formation do not add up. Specifically, they compared the experimentally-determined enthalpy of peptide hydrogen bond formation in an α-helix with the corresponding value derived from a thermodynamic cycle[29]: The two values differ by 7.6 kcal/mol/residue! Their work demonstrates the inadequacy of assuming that a peptide hydrogen bond and a peptide:water hydrogen bond are energetically equivalent. Additionally, they show that short amides, which are dominated by end effects, are deficient models for the longer polypeptide backbone. In summary, their studies reveal that peptide solvation is a complex phenomenon that requires free energy for its accurate evaluation. In their work, Avbelj and Baldwin utilize fitted parameters from the PARSE parameter set,[52] whereas our values are derived from simulations using the CHARMM parameter set. Notably, these disparate methods each give a value of 0.7 kcal/mol/residue for the free energy difference between P_{II} and β-strand (Baldwin, personal communication, vs $\Delta A_{solvation}$ in Table I).

ACKNOWLEDGMENTS

We thank Robert Baldwin, Angel Garcia, Alex Kentsis, and Tobin Sosnick for sharing unpublished manuscripts; and Robert Baldwin, Trevor Creamer, Angel Garcia, Bertrand Garcia-Moreno, Alex Kentsis, Roman Osman, Mike Paulaitis, and Gary Pielak for useful discussion and helpful suggestions. Use of the computer facilities at the Institute of Computational Biomedicine (ICB) of the Mount Sinai Medical Center is gratefully acknowledged.

REFERENCES

1. Tanford C. Protein denaturation. Adv Prot Chem 1968;23:121–282.
2. Flory PJ. Statistical mechanics of chain molecules. New York: Wiley; 1969.
3. Avbelj F, Baldwin RL. Role of backbone solvation in determining thermodynamic beta propensities of the amino acids. Proc Natl Acad Sci USA 2002;99:1309–1313.

4. Avbelj F, Baldwin RL. Role of backbone solvation and electrostatics in generating preferred peptide backbone conformations: distributions of phi. Proc Natl Acad Sci USA 2003;100:5742–5747.
5. Jorgensen WL, Chandrasekhar J, Madura JD, Impey RW, Klein M. Comparison of simple potential functions for simulating liquid water. J Chem Phys 1983;79:926–935.
6. Mezei M. Direct calculation of the excess free energy of the dense Lennard–Jones fluid with nonlinear thermodynamic integration. Mol Simul 1989;2:201–207.
7. Mezei M. Calculation of solvation free energy differences for large solute change from computer simulations with quadrature-based nearly linear thermodynamic integration. Mol Simul 1993;10:225–240.
8. Creamer TP. Left-handed polyproline II helix formation is (very) locally driven. Proteins 1998;33:218–226.
9. Mezei M, Beveridge DL. Structural chemistry of biomolecular hydration via computer simulation; the proximity criterion. Methods Enzymol 1986;127:21–47.
10. McCammon AJ. Computer-aided molecular design. Science 1987; 238:486–491.
11. Straatsma TP, McCammon JA. Computational alchemy. Annu Rev Phys Chem 1992;43:407–435.
12. Mezei M. Polynomial path for the calculation of liquid state free energies from computer simulations tested on liquid water. J Comput Chem 1992;43:651–656.
13. Resat H, Mezei M. Studies in the free energy calculations: I. Thermodynamic integration using a polynomial path. J Chem Phys 1993;99:6052–6061.
14. Mezei M. MMC, Monte Carlo Program: http://inka.mssm.edu/~mezei/mmc.
15. Metropolis N, Rosenbluth AW, Rosenbluth MN, Teller AH, Teller E. Equation of state calculations by fast computing machines. J Chem Phys 1953;21:1087–1092.
16. Rao M, Pangali CS, Berne BJ. Mol Phys 1979;37:1779.
17. Mezei M. Distance-scaled force biased Monte Carlo simulation for solutions containing a strongly interacting solute. Mol Simul 1991;5:405–408.
18. MacKerell J et al. All-atom empirical potential for molecular modeling and dynamics studies of proteins. J Phys Chem B 1998;102:3585–3616.
19. Owicki JC. Computer modeling of matter. In: Lykos PG, Editor. Washington, DC: American Chemical Society; 1978.
20. Mezei M. Simulaid, simulation setup utilities: http://inka.mssm.edu/~mezei/simulaid.
21. Mezei M. Modified proximity criterion for the analysis of the solvation environment of a polyfunctional solute. Mol Simul 1988;1:327–332.
22. Pauling L, Corey RB, Branson HR. The structures of proteins: two hydrogen-bonded helical configurations of the polypeptide chain. Proc Natl Acad Sci USA 1951;37:205–210.
23. Lee B, Richards FM. The interpretation of protein structures: estimation of static accessibility. J Mol Biol 1971;55:379–400.
24. Edsall JT, McKenzie HA. Water and proteins: I. The significance and structure of water: its interaction with electrolytes and non-electrolytes. Adv Biophys 1978;10:137–207.
25. Paulaitis ME, Pratt LR. Hydration theory for molecular biophysics. Adv Prot Chem 2002;62:283–310.
26. Tanford C. The hydrophobic effect: formation of micelles and biological membranes. 2nd edition. New York: Wiley Interscience; 1980.
27. Kauzmann W. Some factors in the interpretation of protein denaturation. Adv Prot Chem 1959;14:1–63.
28. Baldwin RL. Temperature dependence of the hydrophobic interaction in protein folding. Proc Natl Acad Sci USA 1986;83:8069–8072.
29. Avbelj F, Luo P, Baldwin RL. Energetics of the interaction between water and the helical peptide group and its role in determining helix propensities. Proc Natl Acad Sci USA 2000;97: 10786–10791.
30. Dunitz JD. The entropic cost of bound water in crystals and biomolecules. Science 1994;264:670.
31. Hillson N, Onuchic JN, Garcia AE. Pressure-induced protein folding/unfolding kinetics. Proc Natl Acad Sci USA 1999;96:14848–14853.
32. Karle IL Flippen-Anderson J, Uma K, Balaram P. Aqueous channels within apolar peptide aggregates: solvated helix of the alpha-aminoisobutyric acid (Aib)-containing peptide Boc-(Aib-Ala-Leu)3-Aib-Ome · $2H_2O$ · CH_3OH in crystals. Proc Natl Acad Sci USA 1988;85:299–303.
33. Pappu RV, Rose GD. A simple model for polyproline II structure in unfolded states of alanine-based peptides. Protein Sci 2002;11: 2437–2455.
34. Kentsis A, Mezei M, Gindin T, Osman R. Unfolded state of polyalanine is a segmented polyproline II helix. 2003. Submitted for publication.
35. Shi Z, Olson CA, Rose GD, Baldwin RL, Kallenbach NR. Polyproline II structure in a sequence of seven alanine residues. Proc Natl Acad Sci USA 2002;99:9190–9195.
36. Berman HM, Westbrook J, Feng Z, Gilliland G, Bhat TN, Weissig H, Shindyalov IN, Bourne PE. The Protein Data Bank. Nucleic Acids Res 2000;28:235–242.
37. Stapley BJ, Creamer TP. A survey of left-handed polyproline II helices. Protein Sci 1999;8:587–595.
38. Stickle DF, Presta LG, Dill KA, Rose GD. Hydrogen bonding in globular proteins. J Mol Biol 1992;225:1143–1159.
39. Rose GD, Editor. Unfolded proteins [Special issue]. Adv Prot Chem 2002;62.
40. Brandts JF. The thermodynamics of protein denaturation: II. A model of reversible denaturation and interpretations regarding the stability of chymotrypsinogen. J Am Chem Soc 1964;86:4302–4314.
41. Brandts JF. The termodynamics of protein denaturation: I. The denaturation of chymotrypsinogen. J Am Chem Soc 1964;86:4291–4301.
42. Pappu RV, Srinivasan R, Rose GD. The Flory isolated-pair hypothesis is not valid for polypeptide chains: implications for protein folding. Proc Natl Acad Sci USA 2000;97:12565–12570.
43. Tiffany Ml, Krimm S. New chain conformations of poly(glutamic acid) and polylysine. Biopolymers 1968;6:1379–1382.
44. Kelly MA, Chellgren BW, Rucker AL, Troutman JM, Fried MG, Miller AF, Creamer TP. Host–guest study of left-handed polyproline Ii helix formation. Biochemistry 2001;40:14376–14383.
45. Creamer TP, Campbell MN. Determinants of the polyproline II helix from modeling studies. Adv Prot Chem 2002;62:263–282.
46. Rucker AL, Creamer TP. Polyproline II helical structures in protein unfolded states: lysine peptides revisited. Protein Sci 2002;11:980–985.
47. Garcia AE. Characterization of non-alpha helical conformations in Ala peptides. 2003. Submitted for publication.
48. Sreerama N, Woody RW. Molecular dynamics simulations of polypeptide conformations. Proteins 1999;36:400–406.
49. Zaman MH, Shen MY, Berry S, Freed KF, Sosnick TR. Investigations into sequence and conformational dependence of backbone entropy, inter-basin dynamics and the Flory isolated-pair hypothesis for peptides. J Mol Biol 2003;331:693–711.
50. Poon C-D, Samulski ET, Weise CF, Weisshaar JC. Do bridging water molecules dictate the structure of a model dipeptide in aqueous solution? J Am Chem Soc 2000;122:5642–5643.
51. Hinderaker MP, Raines RT. An electronic effect on protein structure. Protein Sci 2003;12:1188–1194.
52. Stikoff D, Sharp KA, Honig B. Accurate calculation of hydration free energies using macroscopic solvent models. J Phys Chem 1994;98:1978–1988.